An Algorithm to Mitigate the Infeed Effect on Overreaching Distance Zones Settings

Kleber M. Silva, *Senior Member, IEEE,* Jéssica S. G. Pena, Helon D. M. Braz, *Member, IEEE,* and Mladen Kezunovic, *Life Fellow, IEEE*

***Abstract*—This paper revisits the analysis of the well-known infeed effect on transmission lines distance protection. A new adaptive algorithm to overcome this drawback is proposed, which requires solely impedance data and the operational status of power apparatus to perform overreaching distance zones settings. A comparison of the proposed strategy and the traditional one is performed. The obtained results demonstrate that the proposed settings ensure the correct operation of overreaching zones. Thereby, the backup coverage is improved significantly, besides avoiding distance zones overlapping between adjacent lines. It reveals the proposed strategy usefulness and value from the practical point of view, since it can be implemented with technology readily available on the market.**

***Index Terms*—Distance protection, infeed current effect, overreaching distance zones.**

I. Introduction

LARGE interconnected grids require bulk power transmission over very long overhead lines. To avoid widespread blackouts, faults must be cleared quick and selectively, requiring various levels of protection system redundancy [1]. Among different redundancy strategies, the use of overreaching distance zones to provide remote backup protection is widespread [2]. Since distance protection suffers from inaccuracies caused by infeed conditions, overreaching zones may underreach and provide smaller backup coverage than expected [3]. This effect can be even worse for transmission lines operating in parts of the grid with large concentration of infeed sources. To overcome this drawback, the infeed effect could be taken into account when settings are determined, but it traditionally requires extensively analysis of system topologies and operational conditions to compute the different infeed currents levels [4]. That is the why infeed effect is usually disregarded during overreaching distance zones setting calculation procedures.

There are some improved algorithms reported on the literature to overcome the infeed effect on distance protection performance [5]–[11]. In [5], the impedance seen by the relay is calculated using a weighted equation whose terms depend on the network parameters. The method described in [6] is based on fault studies, and takes into account single-level contingencies and infeed currents. The new setting strategy presented in [7] uses input signals from local relays along with command data from the distance relay at the remote end transmitted using teleprotection system. In [8], a novel multi-agent system based methodology for power system protection coordination is described. In [9], an adjustment factor is suggested and the probability of a fault being detected correctly when the relay operates is determined. In [10], a synchrophasor-based algorithm, which uses the active power measured on buses to eliminate the effects of infeed currents is reported. In [11], an adaptive setting of the 3rd distance zone based upon synchronized measurements is outlined.

Adaptive strategies for distance protection to update the operating characteristic according to changes in the system topology are proposed in [12]–[19]. In [12], an expert system method to determine the relay settings during power system topology changes is elaborated. In [13], a probabilistic model to adjust all distance zones is developed. In [14], operating characteristics are determined using artificial neural networks. In [15], a new methodology based on the analysis of events and their consequences is discussed. A method based on network mapping obtained using information from the actual system topology is proposed in [16]. In [17], the adequacy of the distance relay settings by comparing the apparent impedance of the actual topology and a pre-defined threshold is evaluated. A wide-area backup protection algorithm that gathers distance relays status is presented in [18]. In [19], a wide-area protection algorithm, defined by an objective function based on the performance of various distance relays zones and telecommunication information is mentioned.

Our paper revisits the infeed effect on transmission lines distance protection and suggests an algorithm to overcome this drawback, by taking into account changes in the system topology. It requires solely impedance data and operational status of power apparatus to determine the overreaching zones settings. It is formulated here for the 2nd zone only, but it can be extended to the 3rd zone straightforwardly. A simplified optimization process is also proposed to improve the backup coverage on adjacent lines. A comparison of the proposed settings and the traditional ones is performed with and without contingencies in a real power system by means of EMTP simulations and experimental tests using a commercial available relay. The obtained results demonstrate that the proposed settings improve the backup protection and also avoids distance zones overlapping in adjacent lines.

This work was supported in part by the Federal District Research Foundation (FAP-DF), in part by Brazilian National Council for Scientific and Technological Development (CNPq) and in part by the Coordination for the Improvement of Higher Education Personnel (CAPES).

Kleber M. Silva and Jéssica S. G. Pena are with the Department of Electrical Engineering at University of Brasilia (UnB), 70910-900 Brasilia, Brazil. (e-mail: klebermelo@unb.br, jessicapena@lapse.unb.br).

Helon David M. Braz. is with the Department of Electrical Engineering at Federal University of Paraiba (UFPB), 58051-970 João Pessoa, Brazil. (e-mail: helon@cear.ufpb.br).

Mladen Kezunovic is with Department of Electrical & Computer Engineering, Texas A&M University, USA. (e-mail: kezunov@ece.tamu.edu)

II. Problem Statement

Consider the general power system topology shown in Fig. 1. The transmission lines starting in buses from ❸ to ⓝ terminate at the bus ❷. For a distance relay located at at bus ⓡ, a solid fault is placed at the fictitious bus ❶, which is inserted in the line between buses ⓜ and ❷. In the example shown in Fig. 1, bus ⓡ is taken as bus ❸, and bus ⓜ corresponds to bus ❹. Thereby, the voltage at the relay point can be computed as [4]:

$$\overline{V}_R = Z_{32}\overline{I}_{32} + hZ_{42}\left(\overline{I}_{32} + \overline{I}_{52} + \cdots + \overline{I}_{N2}\right), \quad (1)$$

where h is the percentage of the line ❹–❷ correspondent to the line segment ❶–❷ (see Fig. 1); Z_{32} and Z_{42} are the series impedance of the lines ❸–❷ and ❹–❷, respectively; and $\overline{I}_{ij}$ is the infeed current coming from the bus ⓘ towards bus ⓙ.

Since the current at the relay point is $\overline{I}_{32}$, the apparent impedance seen by the relay is computed as:

$$Z_R = \frac{\overline{V}_R}{\overline{I}_R} = Z_{32} + hZ_{42}\left(1 + \underbrace{\sum_{n=5}^{N}\frac{\overline{I}_{n2}}{\overline{I}_{32}}}_{M}\right), \quad (2)$$

where M is named as infeed coefficient [4]. Usually, it is a near real positive number, that causes the distance relay to underreach. Traditionally, protection engineers consider some critical operational conditions to include the infeed effect on settings. Nevertheless, since it is challenging to known infeed currents a priory for different operational conditions (i.e., with and without contingencies), there is no guarantee that distance zone overlapping in adjacent lines is completely overcome, mainly for deeply connected power grids. Therefore, for the sake of simplicity, protection engineers may disregard the infeed effect on settings to avoid relay overreaching. As a consequence, the backup coverage on adjacent lines may reduce tremendously depending on infeed current levels [4].

To provide remote backup protection, large 3rd distance zone can be used to cover the adjacent lines entirely [20]. This approach can restrict the amount of load a circuit can carry under emergency conditions due to relays tripping, which leads to an unintentionally operation during widespread disturbances causing cascading relay tripping, as happened in the North American power grid blackout in 2003 [21]. As a result, several countries, among them Brazil, have standardized the use of local backup protection principle for the entire transmission system such that just the 1st and 2nd distance zones have been used.

III. Proposed Algorithm

From (2), and based on the general power system topology shown in Fig. 1, one can write the sequence voltages at the relay point for a fault taking place at bus ❶ in between the line ⓜ-❷, as follows:

$$\overline{V}_{R,m}^{(s)} = Z_{r2}^{(s)}\overline{I}_{r2}^{(s)} + hZ_{m2}^{(s)}\sum_{\substack{n=3\\ n\neq m}}^{N}\overline{I}_{n2}^{(s)}, \quad (3)$$

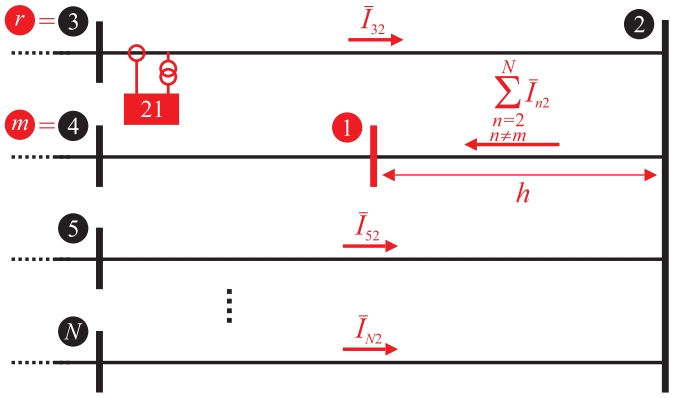

Fig. 1. General power system topology.

where the superscript $(s) = (0)$, (1) or (2) stands for the zero, positive and negative sequence components, respectively; h is the percentage of the line ⓜ–❷ from bus ❶ to bus ❷ (see Fig. 1); $Z_{r2}^{(s)}$ and $Z_{m2}^{(s)}$ are (s)-sequence series impedance of the relay line ⓡ–❷ and the faulted line ⓜ–❷, respectively; and $\overline{I}_{n2}^{(s)}$ is the (s)-sequence infeed current coming from bus ⓝ towards bus ❷, which can be computed as:

$$\overline{I}_{n2}^{(s)} = \frac{\overline{V}_n^{(s)} - \overline{V}_2^{(s)}}{Z_{n2}^{(s)}} = -\left[\frac{z_{n1}^{(s)} - z_{21}^{(s)}}{Z_{n2}^{(s)}}\right]\overline{I}_f^{(s)} = \Gamma_{n2}^{(s)}\overline{I}_f^{(s)}, \quad (4)$$

with

$$\Gamma_{n2}^{(s)} = \frac{z_{n1}^{(s)} - z_{21}^{(s)}}{Z_{n2}^{(s)}}, \quad (5)$$

where $z_{n1}^{(s)}$ and $z_{21}^{(s)}$ stands for the elements $(n,1)$ and $(2,1)$ of the (s)-sequence bus impedance matrix, respectively; $Z_{n2}^{(s)}$ is the (s)-sequence series impedance of the line ⓝ–❷; and $\overline{I}_f^{(s)}$ is the (s)-sequence fault current at the fault point.

Substituting (5) in (3) yields:

$$\overline{V}_{R,m}^{(s)} = \left[Z_{r2}^{(s)} + hZ_{m2}^{(s)}\sum_{\substack{n=3\\ n\neq m}}^{N}\frac{\Gamma_{n2}^{(s)}}{\Gamma_{r2}^{(s)}}\right]\Gamma_{r2}^{(s)}\overline{I}_f^{(s)}. \quad (6)$$

Aiming to understand how phase-to-phase (PP) and phase-to-ground (PG) distance units perform during faults, consider the three-phase and single-phase-to-ground fault analysis discussed next.

A. Phase-to-Phase (PP) Distance Units

In order to analyze the PP distance units response, consider a three-phase fault taking place at the faulted line ⓜ-❷. According to the fault analysis fundamentals [22], $\overline{V}_{R,m}^{(a)} = \overline{V}_{R,m}^{(1)}$ and $\overline{V}_{R,m}^{(b)} = a^2\overline{V}_{R,m}^{(1)}$, such that:

$$\overline{V}_{R,m}^{(a)} - \overline{V}_{R,m}^{(b)} = \left[Z_{r2}^{(1)} + hZ_{m2}^{(1)}\sum_{\substack{n=3\\ n\neq m}}^{N}\frac{\Gamma_{n2}^{(1)}}{\Gamma_{r2}^{(1)}}\right]\left(1 - a^2\right)\Gamma_{r2}^{(1)}\overline{I}_f^{(1)}, \quad (7)$$

where the superscript (a) and (b) stand for phases quantities, and the complex constant $a = 1\angle 120°$. Likewise, $\overline{I}^{(a)}_{R,m} = \overline{I}^{(1)}_{R,m}$ and $\overline{I}^{(b)}_{R,m} = a^2\overline{I}^{(1)}_{R,m}$. Thus, from (4) one can obtain:

$$\overline{I}^{(a)}_{R,m} - \overline{I}^{(b)}_{R,m} = \left(1 - a^2\right)\Gamma^{(1)}_{r2}\overline{I}^{(1)}_{f}. \tag{8}$$

From the distance protection basics, the apparent impedance seen by the phase-to-phase AB unit is computed as [4]:

$$Z^{(ab)}_{R,m} = \frac{\overline{V}^{(a)}_{R,m} - \overline{V}^{(b)}_{R,m}}{\overline{I}^{(a)}_{R,m} - \overline{I}^{(b)}_{R,m}}. \tag{9}$$

Therefore, by substituting (7) and (8) in (9) yields:

$$Z^{(ab)}_{R,m} = Z^{(1)}_{r2} + hZ^{(1)}_{m2}\sum_{\substack{n=3\\ n\neq m}}^{N}\frac{\Gamma^{(1)}_{n2}}{\Gamma^{(1)}_{r2}}, \tag{10}$$

where, one can see that (10) depends on the line impedance and the (s)-sequence bus impedance matrix only.

Similarly, it is possible to determine that for the other phase-to-phase units the response will be the same.

B. Phase-to-Ground (PG) Distance Units

Aiming to analyze the PG distance units response, consider a single-phase-to-ground fault in phase A, taking place at the faulted line m-2. The phase voltage at the relay point can be written as:

$$\begin{aligned}\overline{V}^{(a)}_{R,m} &= \overline{V}^{(0)}_{R,m} + \overline{V}^{(1)}_{R,m} + \overline{V}^{(2)}_{R,m}\\ &= \left[Z^{(0)}_{r2} + hZ^{(0)}_{m2}\sum_{\substack{n=3\\ n\neq m}}^{N}\frac{\Gamma^{(0)}_{n2}}{\Gamma^{(0)}_{r2}}\right]\Gamma^{(0)}_{r2}\overline{I}^{(0)}_{f} +\\ &\quad\left[Z^{(1)}_{r2} + hZ^{(1)}_{m2}\sum_{\substack{n=3\\ n\neq m}}^{N}\frac{\Gamma^{(1)}_{n2}}{\Gamma^{(1)}_{r2}}\right]\Gamma^{(1)}_{r2}\overline{I}^{(1)}_{f} +\\ &\quad\left[Z^{(2)}_{r2} + hZ^{(2)}_{m2}\sum_{\substack{n=3\\ n\neq m}}^{N}\frac{\Gamma^{(2)}_{n2}}{\Gamma^{(2)}_{r2}}\right]\Gamma^{(2)}_{r2}\overline{I}^{(2)}_{f}.\end{aligned} \tag{11}$$

Considering negative sequence impedances are equal to the positive ones, and the relationship of sequence currents at the fault point $\overline{I}^{(0)}_{f} = \overline{I}^{(1)}_{f} = \overline{I}^{(2)}_{f}$, one can rewrite (11) as:

$$\begin{aligned}\overline{V}^{(a)}_{R,m} &= Z^{(1)}_{r2}\overline{I}^{(1)}_{f}\left[2\Gamma^{(1)}_{r2} + (1+K_{r2})\,\Gamma^{(0)}_{r2}\right]\\ &\quad + hZ^{(1)}_{m2}\overline{I}^{(1)}_{f}\sum_{\substack{n=3\\ n\neq m}}^{N}\left[2\Gamma^{(1)}_{n2} + (1+K_{m2})\,\Gamma^{(0)}_{n2}\right],\end{aligned} \tag{12}$$

where $K_{r2} = \dfrac{Z^{(0)}_{r2} - Z^{(1)}_{r2}}{Z^{(1)}_{r2}}$ and $K_{m2} = \dfrac{Z^{(0)}_{m2} - Z^{(1)}_{m2}}{Z^{(1)}_{m2}}$.

From (4) one can obtain:

$$\overline{I}^{(a)}_{R,m} = \overline{I}^{(0)}_{R,m} + \overline{I}^{(1)}_{R,m} + \overline{I}^{(2)}_{R,m} = \Gamma^{(0)}_{r2}\overline{I}^{(0)}_{f} + 2\Gamma^{(1)}_{r2}\overline{I}^{(1)}_{f}. \tag{13}$$

Adding $K_{r2}\overline{I}^{(0)}_{R,m}$ on both sides of (13), it is possible to rewrite (13) as:

$$\overline{I}^{(a)}_{R,m} + K_{r2}\overline{I}^{(0)}_{R,m} = \overline{I}^{(1)}_{f}\left[2\Gamma^{(1)}_{r2} + (1+K_{r2})\,\Gamma^{(0)}_{r2}\right]. \tag{14}$$

From the distance protection basics, the apparent impedance seen by the phase-to-ground AG unit is computed as [4]:

$$Z^{(ag)}_{R,m} = \frac{\overline{V}^{(a)}_{R,m}}{\overline{I}^{(a)}_{R,m} + K_{r2}\overline{I}^{(0)}_{R,m}}. \tag{15}$$

Therefore, by substituting (12) and (14) in (15) yields:

$$Z^{(ag)}_{R,m} = Z^{(1)}_{r2} + hZ^{(1)}_{m2}\sum_{\substack{n=3\\ n\neq m}}^{N}\frac{2\Gamma^{(1)}_{n2} + (1+K_{m2})\,\Gamma^{(0)}_{n2}}{2\Gamma^{(1)}_{r2} + (1+K_{r2})\,\Gamma^{(0)}_{r2}}, \tag{16}$$

where it can be seen that (16) depends on the line impedance and the (s)-sequence bus impedance matrix only.

Likewise, the response of the other phase-to-ground distance units for the different single-phase-to-ground faults can be obtained straightforwardly in the same.

C. 2nd Zone Settings for PP and PG Distance Units

Considering faults in the different lines connected to the bus 2, and varying the percentage h of the faulted line (see Fig. 1), one can calculate the 2nd zone setting Z^{PP}_{2nd} of PP distance units using (10). Thereby, the effective backup protection coverage $C^{PP}_{R,m}$ for faults in the different lines can be obtained taking into account the infeed effect by solving:

$$Z^{PP}_{2nd} = \underbrace{Z^{(1)}_{r2} + C^{PP}_{R,m}Z^{(1)}_{m2}G^{PP}_{R,m}}_{Z^{PP}_{R,m}}, \tag{17}$$

where $Z^{PP}_{R,m}$ is the apparent impedance seen by the PP distance unit of the relay for a fault taking place at the percentage $C^{PP}_{R,m}$ of the line m-2; $m \neq r$ and the coefficient $G^{PP}_{R,m}$ is computed as:

$$G^{PP}_{R,m} = \sum_{\substack{n=3\\ n\neq m}}^{N}\frac{\Gamma^{(1)}_{n2}}{\Gamma^{(1)}_{r2}}. \tag{18}$$

Thereby, the total effective backup protection coverage for all the adjacent lines connected to bus 2 can be obtained as:

$$TC^{PP}_{R,m} = \sum_{\substack{m=3\\ m\neq r}}^{N} C^{PP}_{R,m}. \tag{19}$$

According to (16), one can calculate the 2nd zone setting Z^{PG}_{2nd} for PG distance units taking into account the infeed effect, considering phase-to-ground faults in the different lines connected to the bus 2, and changing the percentage h where the fault may occur. Thus, the effective coverage $C^{PG}_{R,m}$ for faults in different lines can be determined as:

$$Z^{PG}_{2nd} = \underbrace{Z^{(1)}_{r2} + C^{PG}_{R,m}Z^{(1)}_{m2}G^{PG}_{R,m}}_{Z^{PG}_{R,m}}, \tag{20}$$

where $Z^{PG}_{R,m}$ is the apparent impedance seen by the PG distance unit of the relay for a phase-to-ground fault taking place at the percentage $C^{PP}_{R,m}$ of the line m-2; $m \neq r$ and the coefficient $G^{PG}_{R,m}$ is computed as:

$$G^{PG}_{R,m} = \sum_{\substack{n=3\\ n\neq m}}^{N}\frac{2\Gamma^{(1)}_{n2} + (1+K_{m2})\,\Gamma^{(0)}_{n2}}{2\Gamma^{(1)}_{r2} + (1+K_{r2})\,\Gamma^{(0)}_{r2}}. \tag{21}$$

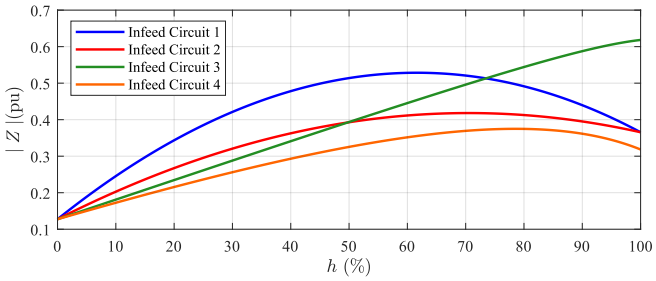

Fig. 2. Proposed settings versus boundary buses impedances variations.

Thus, the total effective percentage coverage for all the adjacent lines connected to bus ❷ can be determined as:

$$TC_{R,m}^{PG} = \sum_{\substack{m=3 \\ m \neq r}}^{N} C_{R,m}^{PG}. \tag{22}$$

It is noteworthy that, for both PP and PG distance units, $G_{R,m}$ depends on $C_{R,m}$ and this relation might be quite nonlinear, specially for deeply connected power grids. It is observed in Fig. 2, that shows some apparent impedance curves seen by the relay for different adjacent lines. Therefore, different strategies could be used to solve (17) and (20), obtaining the effective backup coverage $C_{R,m}$ related to Z_{2nd}. Traditionally, when infeed effect is taken into account during settings calculation, protection engineers use short-circuit programs to compare $|Z_{R,m}|$ and $|Z_{2nd}|$ graphically for some critical operational conditions known beforehand. The load current are usually disregarded. Thereby, Z_{2nd} is obtained to mitigate distance zones overlapping [4]. Nevertheless, even though this method is widespread, its use in an automatic procedure to compute the effective coverage considering all the system topologies may lead to large errors, because for meshed grids the fault current direction may change throughout the system depending on the fault location. As a result, $|Z_{R,m}|$ may be smaller than $|Z_{2nd}|$, but $Z_{R,m}$ is outside of the distance operation characteristic. To overcome this drawback, alternatively, in our paper we evaluate whether $Z_{R,m}$ lies inside the operation characteristic using cosine-type phase comparators [22]. Thereby a more reliable estimation of $C_{R,m}$ can be obtained, because the comparator output is more similar to that of commercial available relays.

To define the best relay settings Z_{2nd}^{PP} and Z_{2nd}^{PG}, a simplified optimization method is applied: the sum of backup coverage in the all adjacent lines is maximized and restricted to a specified maximum coverage of an adjacent line in particular, to avoid distance zones overlapping.

D. Simplified Optimization Process

For the sake of simplicity, superscripts PP and PG are omitted, since the same optimization process is applied for both units. The goal is to calculate the percentage h_m in the adjacent line ⓜ-❷ used to compute the 2nd zone settings that maximize the effective backup coverage for all adjacent lines, subject to the given constraint C_{max}, which stands for the maximum coverage considered for backup protection.

The premise taken is that, for the k-th iteration, $h_{m,k}$ has a polynomial relation with the maximum backup coverage $C_{m,k}$ among the adjacent lines. Therefore, a second order Lagrange interpolation polynomial has been applied as follows [23]:

$$\begin{aligned} h_{m,k} = & \frac{(1-C_{m,k-2})}{(C_{m,k-3}-C_{m,k-2})}\frac{(1-C_{m,k-1})}{(C_{m,k-3}-C_{m,k-1})}h_{m,k-3} \\ & + \frac{(1-C_{m,k-3})}{(C_{m,k-2}-C_{m,k-3})}\frac{(1-C_{m,k-1})}{(C_{m,k-2}-C_{m,k-1})}h_{m,k-2} \\ & + \frac{(1-C_{m,k-3})}{(C_{m,k-1}-C_{m,k-3})}\frac{(1-C_{m,k-2})}{(C_{m,k-1}-C_{m,k-2})}h_{m,k-1}. \end{aligned} \tag{23}$$

The 2nd distance zone setting is computed for $h_{m,k}$ [using (10) or (16)], and its effective backup coverage for each adjacent line is calculated [using (17) or (20)]. Thereby, $C_{m,k}$ is taken as the largest backup coverage among adjacent lines, creating an ordered pair $(h_{m,k}, C_{m,k})$. Then (23) is applied to $k+1$, and so on. The optimization process continues until the optimal $h_{m,k}$ is obtained subject to the constraint C_{max}.

Special countermeasures must be taken for $k \leq 2$: for $k = 0$, $(h_{m,0}, C_{m,0}) = (0, 0)$ and for $k = 1$, $h_{m,1}$ is assumed equal to a initialization value h_{ini} arbitrarily. Then, the 2nd distance zone setting is computed for h_{ini}, and the maximum backup coverage $C_{m,1}$ is taken as the largest coverage among adjacent lines, creating the ordered pair $(h_{m,1}, C_{m,1})$. For $k = 2$, in turn, the percentage $h_{m,2}$ is calculated using the first order Lagrange polynomial as [23]:

$$h_{m,2} = \frac{1}{C_{m,1}} h_{m,1}. \tag{24}$$

Then, the 2nd zone setting is computed, and the maximum backup coverage $C_{m,2}$ is taken as the largest effective coverage in adjacent lines, creating the ordered pair $(h_{m,2}, C_{m,2})$.

In order to avoid convergence problems, $h_{m,k}$ for each iteration must be confined to a limit defined as:

$$h_{m,k-1} - \Delta h_{max} < h_{m,k} < h_{m,k-1} + \Delta h_{max}, \tag{25}$$

where Δh_{max} is the maximum increment considered.

At the end of the whole optimization process, the optimal h_m and its correspondent 2nd zone setting for each adjacent line are obtained, as well as their effective backup coverage in each circuit.

The proposed settings Z_{2nd}^{PP} and Z_{2nd}^{PG} are those that lead to the largest total effective percentage coverage, which are computed using (19) for PP units and using (22) for PG units.

E. Proposed Algorithm Application

As one can see, the proposed algorithm requires only impedance data and the operational status of the power apparatus. Then, the simplified optimization process described in the Sec. III-D can be carried out, resulting in the optimal 2nd zone settings that lead to the maximum backup protection coverage for adjacent lines. It can be used for both offline and online applications straightforwardly.

For offline applications, the proposed algorithm gives support to protection engineers, providing optimal settings calculation. Contingency scenarios of nearby equipment can be

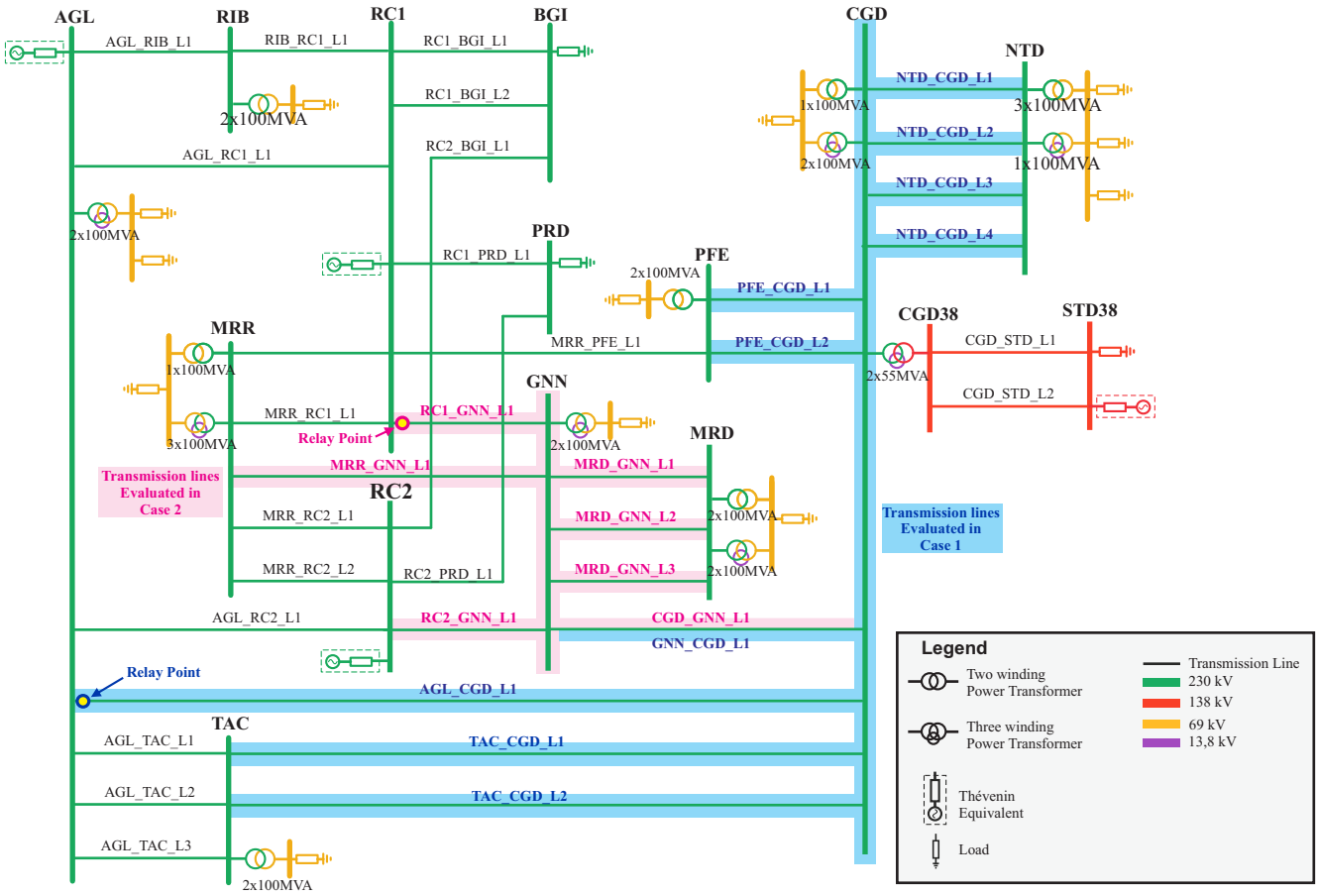

Fig. 3. Evaluated Power System.

considered during the optimization process to prevent 2nd zone overlapping of adjacent lines. Moreover, permanent topology changes may occur over time, and new apparatus may be connected to the grid. The proposed algorithm can also be used to monitor the effectiveness of distance relays settings continuously.

Following the concept of wide-area adaptive protection applications, the proposed algorithm can also be integrated into a feedback loop toward relays to change their settings online dynamically. Aiming to do so, the operational status of the power apparatus provided by SCADA can be used to decide whether relay settings must be updated. Moreover, it is noteworthy that it must be done only for those contingencies that lead to large overreach and may cause 2nd zone overlapping in adjacent lines, as discussed next.

IV. Proposed Algorithm Evaluation

Aiming to evaluate the proposed algorithm, the power system depicted in Fig. 3 was modeled in software ATP/ATPDraw. It corresponds to part of the power system of a Brazilian utility. Power transformers were represented using the saturable transformer model, and transmission lines were modeled as fully transposed using the Bergeron model [24]. Load and shunt reactors were modelled as lumped components. Thévenin's equivalents were included in boundary buses (i.e., AGL, RC1 and RC2), considering both self and mutual impedances. Then, power equipment impedance data were used to calculate the 2nd distance zone setting by means of the proposed algorithm. Finally, faults were simulated using ATP/ATPDraw to assess the actual backup coverage performance of the obtained settings.

Settings obtained by the proposed algorithm consider the maximum constraint of 60% (i.e., $C_{max} = 0.6$) for the effective backup coverage. Their results were compared to those calculated using the traditional procedure, without taking into account infeed effect and considering 30% of the impedance of the smallest adjacent line [4]. Two different cases were evaluated. In each one, the effective coverage of both PP and PG units were computed for each infeed circuit, with and without contingencies in the system. Then, faults were simulated in ATP/ATPDraw using time step of 1 μs, exactly on the maximum backup coverage zone obtained using the proposed algorithm for each infeed circuit. A third order low-pass anti-aliasing Butterworth filter with cutoff frequency at 180 Hz was applied to voltages and currents at the relay point (see Fig. 3). The filtered signals were resampled at 16 samples per cycle of 60 Hz, and then phasors were estimated [25]. The apparent impedance seen by the relay for each distance unit is shown in the RX diagram along with Mho characteristics of 2nd distance zones adjusted using proposed settings and the traditional ones. As another test, ATP/ATPDraw simulated signals were converted into COMTRADE files, thereby exper-

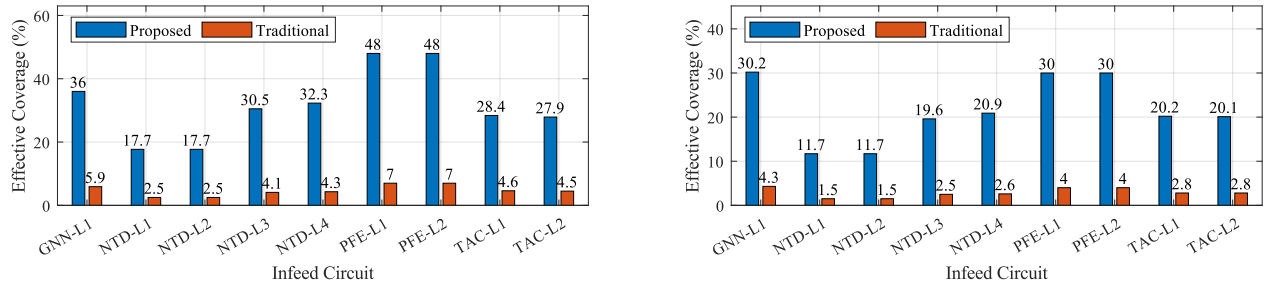

(a) (b)

Fig. 4. Case 1 – Effective coverage obtained by the proposed and traditional settings considering the system without contingency: (a) PP units; (b) PG units.

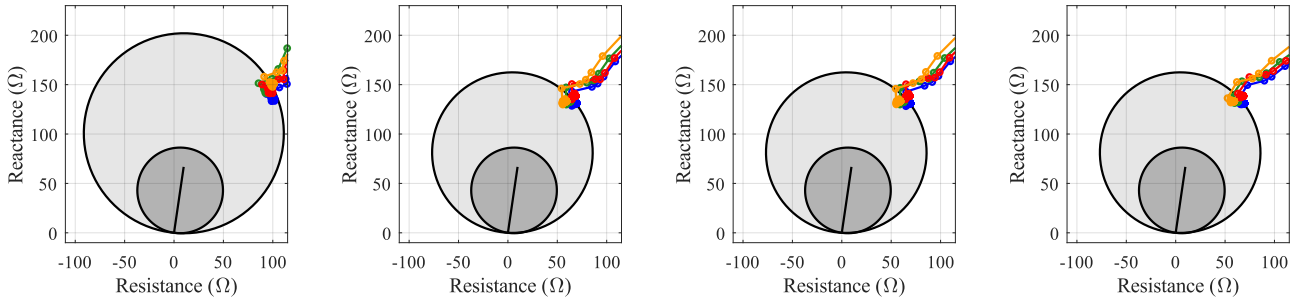

(a) (b) (c) (d)

Fig. 5. Case 1 – Performance comparison of 2nd distance zone settings computed using the proposed algorithm and the traditional procedure, considering different types of faults: (a) AG, (b) BC, (c) BCG and (d) ABC.

imental evaluation were carried out using a playback test with a commercial available relay.

A. Case 1

In Case 1, lines from buses AGL, GNN, NTD, PFE, and TAC to the bus CGD were considered (see transmission lines highlighted in blue color on Fig. 3). In this case, the relay is located at the terminal AGL of the transmission line AGL_CGD_L1.

The proposed algorithm was applied to the system topology shown in Fig. 3, without contingencies. It converged in 65 iterations for PP units and in 61 iterations for PG units. The effective coverage obtained using the proposed and traditional settings are illustrated in Fig. 4(a) and 4(b) for PP and PG units, respectively. As one can see, the proposed settings lead to much larger backup coverage of adjacent lines. Indeed, as discussed in Sec. II, since the traditional procedure evaluated here disregard the infeed effect, and bus CGD concentrates a large number of circuits, the backup coverage provided by the traditional settings is quite reduced.

The performance of the distance relay for faults simulated using ATP/ATPDraw are shown in Figs. 5. Each color used to plot the apparent impedance represents results for a fault simulated in a particular adjacent line, exactly on the maximum backup coverage computed using the proposed algorithm [see Figs. 4(a) and 4(b)]. For example, the blue color is used to plot the apparent impedance seen by the relay for faults in the line TAC_CGD_L1, whereas the green color is taken for faults in the line GNN_CGD_L1, and so on. The light gray Mho characteristic represents the 2nd distance zone obtained using the proposed settings, whereas the dark one was adjusted using the traditional procedure. In Fig. 5(a), the apparent impedance computed by the ZAG distance unit for an AG solid fault is shown. On the other hand, Figs. 5(b) and 5(c) depict the apparent impedance seen by the ZBC distance unit for BC and BCG solid faults, respectively. Fig 5(d), in turn, shows the apparent impedance seen by the ZAB distance unit for a three-phase solid fault. As it can be observed, the apparent impedance settled down on the light gray Mho characteristic boundary in all cases, revealing the proposed settings improves distance protection performance. Conversely, if traditional settings procedure is used, the relay underreaches and does not provide effective backup protection.

Aiming to further evaluate the effectiveness of the proposed and traditional settings, the contingency of each infeed circuit was assessed, and then the backup protection coverage in the remain circuits were computed. The obtained results are shown in Figs. 6(a) and 6(b) for PP units, respectively, whereas the results for PG units are shown in Figs. 7(a) and 7(b), respectively. These figures depict the percentage coverage matrices for contingency analysis. Their rows represent the effective coverage of the relay settings for infeed circuits, regarding one of them is under contingency. For example, the first row of matrices shown in Figs. 6 and 7 represents the effective coverage of the proposed and traditional settings for each infeed circuit, considering the line TAC_CGD_L1 is under contingency. Whenever the effective coverage is smaller than the maximum constraint of 60%, the correspondent cell is filled in green color. Otherwise, cells are filled in red color, indicating the maximum constraint was violated, except the main diagonal cells, in which a blue color and the letter X were used to represent these elements must be disregarded.

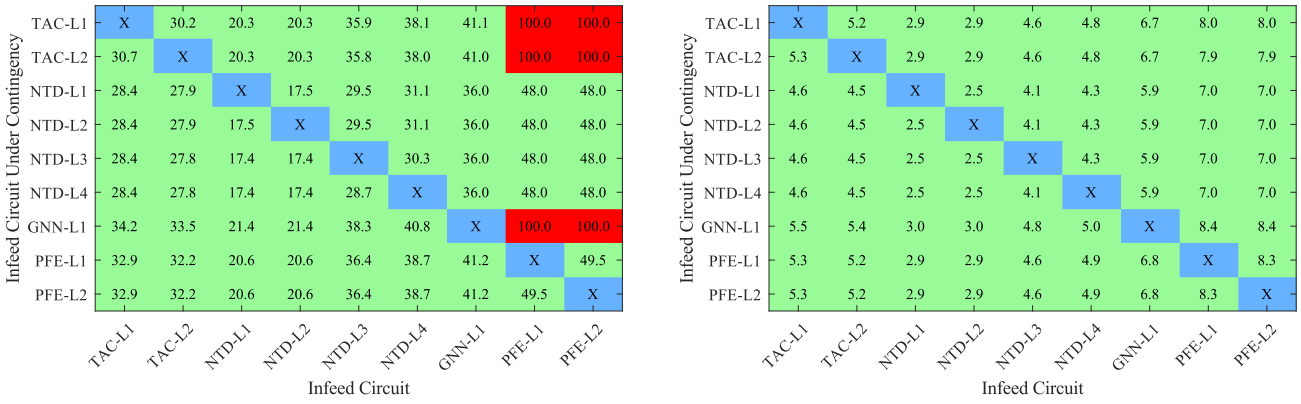

Fig. 6. Case 1 – Percentage coverage matrix for PP distance units in the case of a single contingency on infeed circuits: (a) proposed settings computed without considering contingencies; (b) traditional settings.

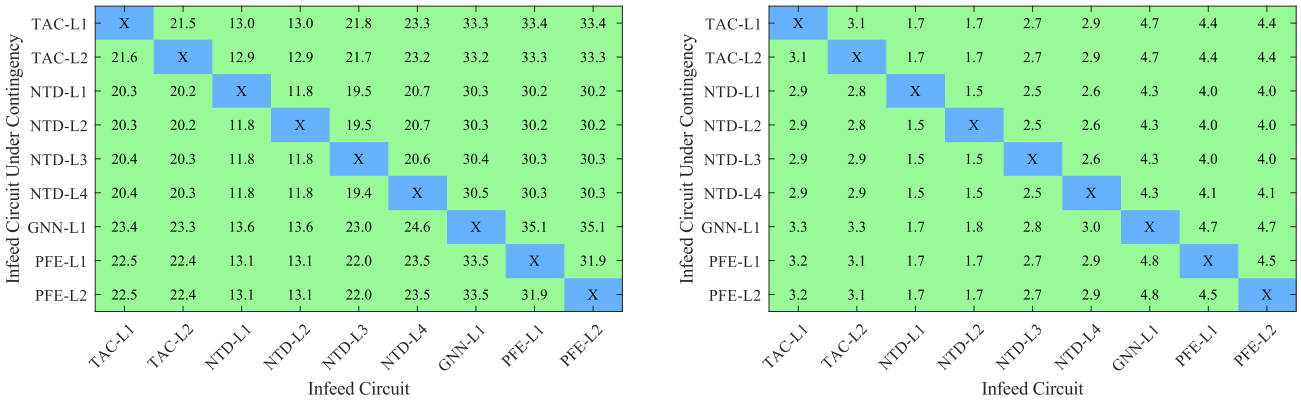

Fig. 7. Case 1 – Percentage coverage matrix for PG distance units in the case of a single contingency on infeed circuits: (a) proposed settings computed without considering contingencies; (b) traditional settings.

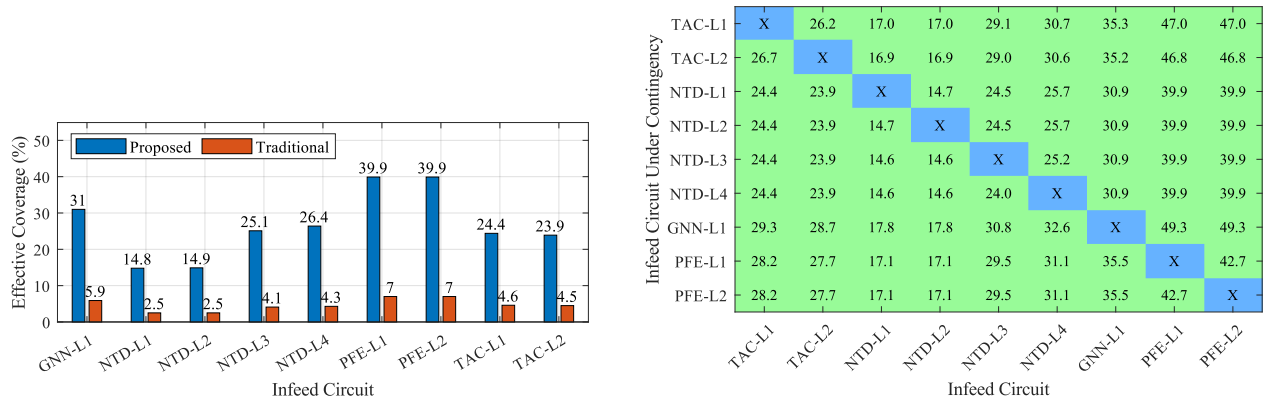

Fig. 8. Case 1 – Results of the new proposed setting for PP units considering contingencies during the optimization process: (a) effective coverage for the system without contingency (b) percentage coverage matrix in the case of contingencies on infeed circuits.

By the analysis of Fig. 6(a), one can see that the proposed settings lead to quite larger effective coverage for PP distance units in comparison with the traditional ones. However, they overreach remote bus of adjacent lines during contingencies in lines TAC_CGD_L1, TAC_CGD_L2 and GNN_CGD_L1, revealing this setting must be updated. In offline applications, contingencies could be taken into account during the optimization process, resulting new settings that avoid 2nd zones overlapping. The effective coverage obtained using this new setting for PP units are illustrated in Fig. 8(a), and the correspondent percentage coverage matrix is shown in Fig. 8(b). As observed, the overreach was completely overcome, and the effective coverage of the proposed setting is still quite larger than the one obtained using the traditional setting. Alter-

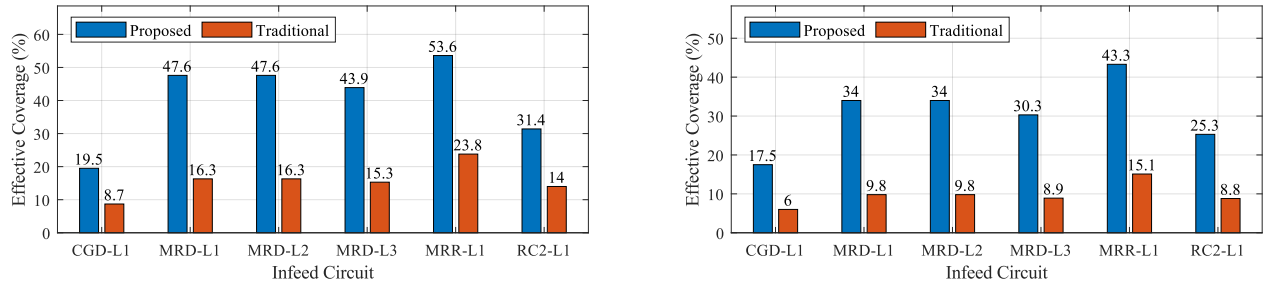

Fig. 9. Case 2 – Effective coverage obtained by the proposed and traditional settings considering the system without contingency: (a) PP units; (b) PG units.

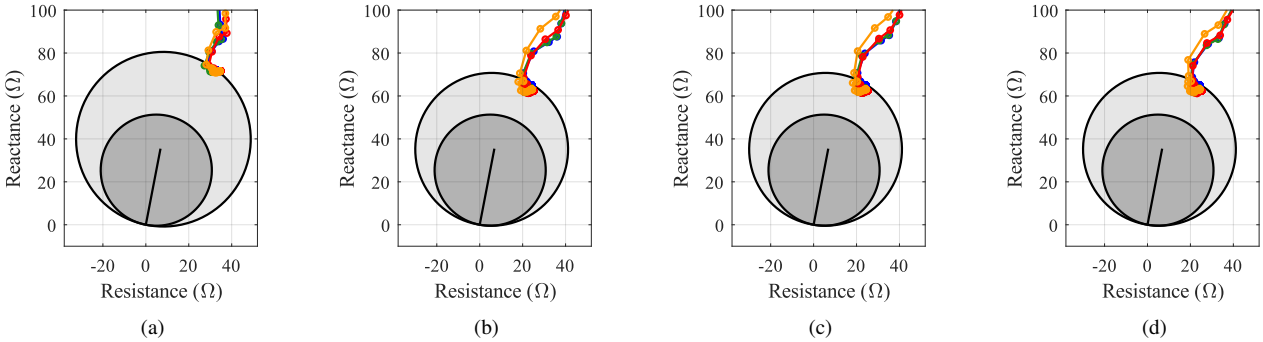

Fig. 10. Case 2 – Performance comparison of 2nd distance zone settings computed using the proposed algorithm and the traditional procedure, considering different types of faults: (a) AG, (b) BC, (c) BCG and (d) ABC.

natively, an adaptive protection scheme could be implemented for online applications. Therefore, whenever contingencies in lines TAC_CGD_L1, TAC_CGD_L2 and GNN_CGD_L1 are detected by the analysis of SCADA data, new settings for the system operating with each one of them out of service could be send to the relay. Also, since these scenarios are known beforehand, settings could be computed offline. Thereby, one can understand that the proposed settings could always provide the optimal backup protection coverage.

Conversely, besides the proposed setting for PG units lead to larger backup protection coverage than the traditional setting, there is no overreach larger than 60%, even when contingencies in infeed circuits happens. Therefore, in the case of PG units, the proposed setting computed without taking into consideration contingencies does not need to be updated.

B. Case 2

In Case 2, lines from buses RC1, RC2, CGD, MRR and MRD to the bus GNN were considered (see transmission lines highlighted in pink color on Fig. 3). In this case, the relay is located at the terminal RC1 of the line RC1_GNN_L1.

The proposed algorithm was applied to the system topology shown in Fig. 3, without considering contingencies. It converged in 61 iterations for PP units and in 54 iterations for PG units. The effective coverage obtained using the proposed settings and the traditional ones are illustrated in Fig. 9(a) and 9(b) for PP and PG units, respectively. As one can see, the proposed settings lead to larger backup coverage of adjacent lines (at least the double in all cases).

The performance of the distance relay for faults simulated using ATP/ATPDraw are shown in Figs. 10. Each color used to plot the apparent impedance represents results for a fault simulated at the maximum backup coverage computed using the proposed algorithm for each adjacent line. For example, the blue color is used to plot the apparent impedance seen by the relay for faults in the line RC2_GNN_L1, whereas the green color is taken for faults in the line CGD_GNN_L1, and so on. The light gray Mho characteristic represents the 2nd distance zone obtained using the proposed settings, whereas the dark one was adjusted using the traditional settings. In Fig. 10(a), the apparent impedance computed by the ZAG distance unit for an AG solid fault is shown. On the other hand, Figs. 10(b) and 10(c) depict the apparent impedance seen by the ZBC distance unit for BC and BCG solid faults, respectively. Fig 10(d), in turn, shows the apparent impedance seen by the ZAB distance unit for a three-phase solid fault. As it can be observed, the apparent impedance settled down on the light gray Mho characteristic boundary in all cases, revealing the proposed settings improves distance protection performance. Conversely, if the traditional settings procedure is used, the relay underreaches and does not provide effective backup protection.

The percentage coverage matrices for contingency analysis of the proposed and traditional settings are shown in Figs. 11(a) and 11(b) for PP distance units, respectively, whereas the ones for PG units are shown in Figs. 12(a) and 12(b), respectively. It can be seen that the proposed settings lead to larger effective coverage for both PP and PG units in comparison with the traditional settings. However, both units overreach remote bus of adjacent lines during contingencies in lines RC2_GNN_L1, CGD_GNN_L1 and MRR_GNN_L1, revealing these settings must be updated. In offline applica-

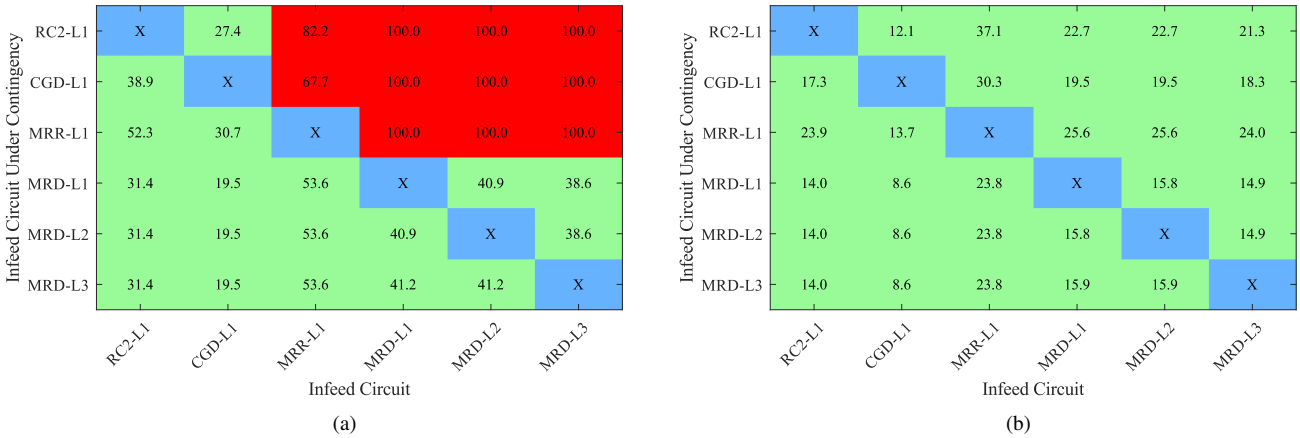

Fig. 11. Case 2 – Percentage coverage matrix for PP distance units in the case of a single contingency on infeed circuits: (a) proposed settings computed without considering contingencies; (b) traditional settings.

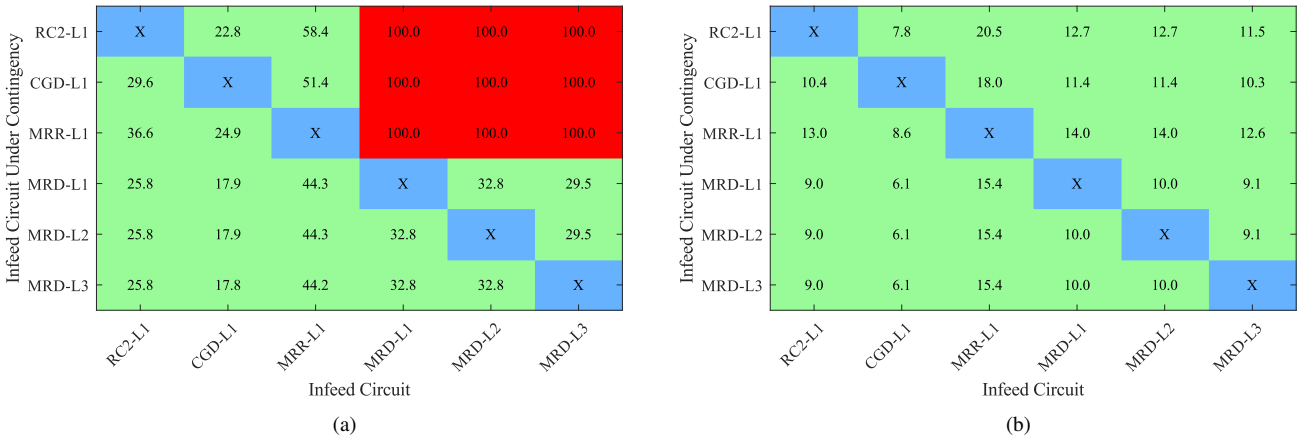

Fig. 12. Case 2 – Percentage coverage matrix for PG distance units in the case of a single contingency on infeed circuits: (a) proposed settings computed without considering contingencies; (b) traditional settings.

tions, contingencies could be taken into account during the optimization process, resulting in new settings that avoid 2nd zones overlapping. The backup coverage obtained using this new setting for PP and PG units are illustrated in Figs. 13(a) and 13(b), respectively. The correspondent percentage coverage matrices are shown in Figs. 14(a) and 14(b), respectively. As observed, the overreach was overcome for both PP and PG units and the effective coverage of the proposed settings is still larger than the one obtained using the traditional settings. Alternatively, an adaptive protection scheme could be implemented for online applications. Therefore, whenever contingencies in lines RC2_GNN_L1, CGD_GNN_L1 and MRR_GNN_L1 are detected by the analysis of SCADA data, new settings previously calculated offline for the system with each one of them out of service could be send to the relay. Thereby, the proposed settings could always provide the optimal backup protection coverage, besides avoiding 2nd zone overlapping.

C. Boundary Buses Impedances Influence

Aiming to evaluated the impact of impedances of boundary buses on the proposed settings, a sensitivity analysis was carried out. In each case, Thévenin equivalent impedances in the boundary buses AGL, RC1 and RC2 (see Fig. 3) were varied from -50% to $+50\%$, and the magnitude variation on settings obtained using the proposed algorithm for both PP and PG units was observed, as shown in Fig. 15. As demonstrated, even with a quite large variation of impedances in the boundary buses, the variation on settings ranges between $\pm 1.35\%$. Indeed, as a rule of thumb, it is recommended that monitored system boundaries are defined two buses away from the relay bus whenever it is possible. Thereby, these equivalents have no significant influence on the proposed settings so their impact can be disregarded and their values for just one specific operational condition are required (e.g., for heavy load condition). Admittedly, the impedance data and operational status of power equipment in the monitored system are more important to the proposed algorithm.

D. Experimental Evaluation

The performance of the proposed settings was also evaluated in a commercially available relay, considering case 1 and 2 described in Sec. IV-A and IV-B. To prove the usefulness of the proposed method, quadriletaral characteristic was used for both PP and PG 2nd distance units instead of mho characteristic. To do so, only reactances of the proposed settings and the

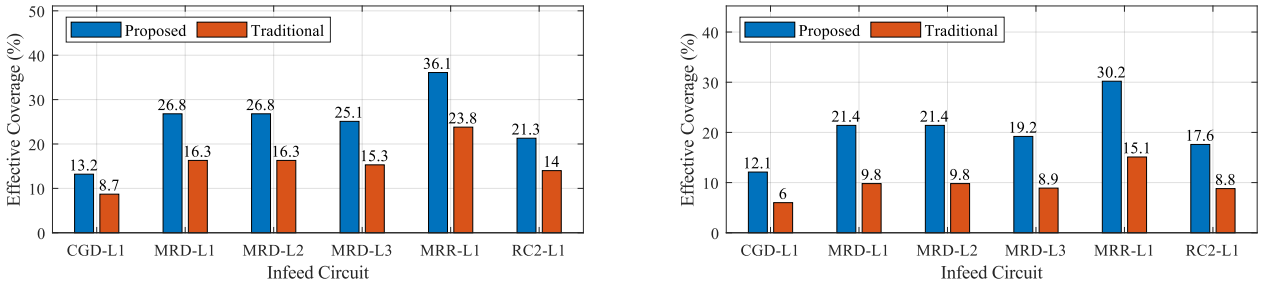

(a) (b)

Fig. 13. Case 2 – Effective coverage of the proposed settings, considering contingencies on infeed circuits, and of the traditional settings: (a) PP distance units; (b) PG distance units.

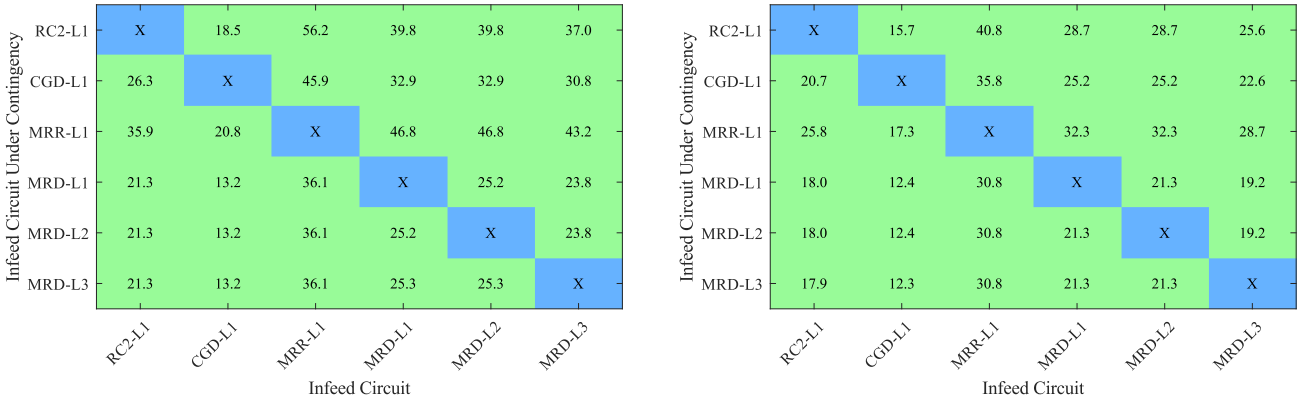

(a) (b)

Fig. 14. Case 2 – Percentage coverage matrix for the proposed settings computed considering contingencies on infeed circuits: (a) PP distance unit; (b) PG distance unit.

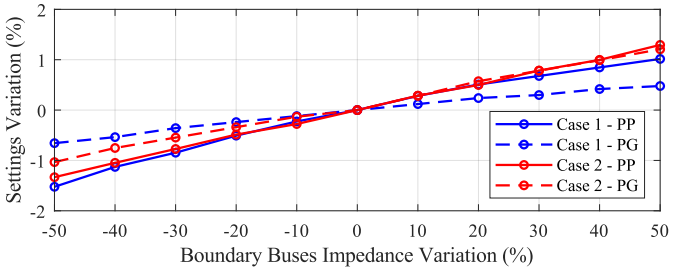

Fig. 15. Proposed settings versus boundary buses impedances variations.

traditional ones were taken into account. The ATP/ATPDraw simulated signals were converted in COMTRADE files and a playback test was carried out using a conventional relay test set. The obtained results reaffirmed the computer simulations, such that all faults were detected only when the proposed settings were used, guaranteeing the maximum backup coverage for each adjacent lines.

V. Conclusions

In this paper, the well-known infeed effect on distance protection was revisited and an adaptive algorithm to compute 2nd distance zone settings was proposed. It requires only impedance data and operational status of power apparatus, such that voltages and currents are not required. It can be used for both offline and online applications straightforwardly.

For offline applications, the proposed algorithm gives support to protection engineers, providing optimal settings calculation. Outage scenarios in nearby equipment can be taken into account during the optimization process. On the other hand, it can also be used for online applications in the context of wide-area adaptive protection schemes. Aiming to do so, the relay can change its settings depending on whether contingencies are detected by SCADA data analysis. It is noteworthy that the settings only need to be changed if contingency takes place in a few infeed circuits. Since these scenarios are known beforehand, settings could be computed offline. Moreover, there is no need to make changes for contingencies in faraway lines. Thereby, one can understand that the proposed settings could always provide the maximum backup coverage for each adjacent line.

It is noteworthy that the proposed method disregards the load current effect, likewise the settings procedure traditionally used by protection engineers. As a result, admittedly, the distance protection function may underreach or overeach, depending on the the loading condition. To overcome this drawback, the proposed algorithm could be improved by taking into account the loading current. Furthermore, the proposed method proposes a correction on the 2nd zone settings, rather than distance polarizing quantities (e.g, zero and negative sequence quantities), what could improve even more the distance function performance. Indeed, such improvements will be presented in future researches.

The effectiveness of the proposed algorithm was assessed by means of faults simulated in an actual power system of a Brazilian utility using ATP/ATPDraw software. The apparent impedance seen by the relay algorithm for each case was plotted in the RX diagram along with Mho characteristics of 2nd distance zones adjusted using the proposed settings and traditional settings. It was observed that the apparent impedance settled down on the Mho characteristic boundary adjusted using proposed settings in all cases, revealing the proposed algorithm improves tremendously the backup protection coverage by taking the infeed effect into account, while avoiding distance zones overlapping between adjacent lines. The same results were observed in the experimental evaluation using a commercially available relay. This highlights the proposed algorithm usefulness and value from the practical point of view, since it can be implemented with the digital technology readily available on the market.

REFERENCES

[1] IEEE PSRC Working Group I19, "Redundancy considerations for protective relaying systems," USA, Tech. Rep., 2019.

[2] IEEE PSRC Working Group D4, "Application of overreaching distance relays," USA, Tech. Rep., 2009.

[3] W. A. Elmore, *Protective Relaying Theory And Applications*. New York, US: CRC Press, 2003.

[4] G. Ziegler, *Numerical Distance Protection: Principles and Applications*, 2nd ed. Berlin, Germany: Siemens, 2006.

[5] Y. Xia, K. Li, and A. David, "Adaptive relay setting for stand-alone digital distance protection," *IEEE Transactions on Power Delivery*, vol. 9, no. 1, pp. 480–491, 1994.

[6] T. Sidhu, D. Baltazar, R. Palomino, and M. Sachdev, "A new approach for calculating zone-2 setting of distance relays and its use in an adaptive protection system," *IEEE Transactions on Power Delivery*, vol. 19, no. 1, pp. 70–77, 2004.

[7] M. Gilany, A. M. Al-Kandari, and J. Madouh, "A new strategy for determining fault zones in distance relays," *IEEE Transactions on Power Delivery*, vol. 23, no. 4, pp. 1857–1863, 2008.

[8] M. A. Haj-ahmed and M. S. Illindala, "Intelligent coordinated adaptive distance relaying," *Electric Power Systems Research*, vol. 110, pp. 163–171, 2014.

[9] J. Ma, C. Liu, and J. S. Thorp, "A wide-area backup protection algorithm based on distance protection fitting factor," *IEEE Transactions on Power Delivery*, vol. 31, no. 5, pp. 2196–2205, 2016.

[10] N. A. Al-Emadi, A. Ghorbani, and H. Mehrjerdi, "Synchrophasor-based backup distance protection of multi-terminal transmission lines," *IET Gen., Trans. & Distrib.*, vol. 10, no. 13, pp. 3304–3313, 2016.

[11] P. Regulski, W. Rebizant, M. Kereit, and S. Schneider, "Adaptive reach of the 3rd zone of a distance relay with synchronized measurements," *IEEE Transactions on Power Delivery*, vol. 36, no. 1, pp. 135–144, 2021.

[12] J. Wang and J. Trecat, "Rsvies-a relay setting value identification expert system," *Elec. Pow. Sys. Research*, vol. 37, no. 2, pp. 153–158, 1996.

[13] J. Pinto De Sa, J. Afonso, and R. Rodrigues, "A probabilistic approach to setting distance relays in transmission networks," *IEEE Transactions on Power Delivery*, vol. 12, no. 2, pp. 681–686, 1997.

[14] K. Li, L. Lai, and A. David, "Stand alone intelligent digital distance relay," *IEEE Trans. Power Systems*, vol. 15, no. 1, pp. 137–142, 2000.

[15] K. El-Arroudi, G. Joos, D. McGillis, and R. Brearley, "Comprehensive transmission distance protection settings using an intelligent-based analysis of events and consequences," *IEEE Transactions on Power Delivery*, vol. 20, no. 3, pp. 1817–1824, 2005.

[16] P. Kundu and A. K. Pradhan, "Enhanced protection security using the system integrity protection scheme (sips)," *IEEE Transactions on Power Delivery*, vol. 31, no. 1, pp. 228–235, 2016.

[17] M. Tasdighi and M. Kezunovic, "Automated review of distance relay settings adequacy after the network topology changes," *IEEE Transactions on Power Delivery*, vol. 31, no. 4, pp. 1873–1881, 2016.

[18] M. Chen, H. Wang, S. Shen, and B. He, "Research on a distance relay-based wide-area backup protection algorithm for transmission lines," *IEEE Transactions on Power Delivery*, vol. 32, no. 1, pp. 97–105, 2017.

[19] S. A. E. Mousavi, R. M. Chabanloo, M. Farrokhifar, and D. Pozo, "Wide area backup protection scheme for distance relays considering the uncertainty of network protection," *Electric Power Systems Research*, vol. 189, p. 106651, 2020.

[20] NERC Report - System Protection and Control Task Force, "Rationale for the use of local and remote (zone 3) protective relaying backup systems," Princeton, NJ, EUA, Tech. Rep., 2005.

[21] NERC Steering Group Report, "Technical analysis of the august 14, 2003, blackout: What happened, why, and what did we learn?" Princeton, NJ, EUA, Tech. Rep., 2004.

[22] P. M. Anderson, *Power System Protection*. Piscataway, New Jersey, EUA: John Wiley & Sons Inc., 1999.

[23] W. H. Press, S. A. Teukolsky, W. T. Vetterling, and B. P. Flannery, *Numerical Recipes: The Art of Scientific Computing*. Cambridge, UK: Cambridge University Press, 2007.

[24] *ATP - Alternative Transient Program*, Leuven EMTP Center, Herverlee, Belgium, 1987.

[25] K. M. Silva and F. A. O. Nascimento, "Modified dft-based phasor estimation algorithms for numerical relaying applications," *IEEE Trans. on Power Delivery*, vol. 33, no. 3, pp. 1165–1173, Jun. 2018.

Kleber M. Silva (M'05, SM'20) received the B.Sc., M.Sc., and Ph.D. degrees in electrical engineering from the University of Campina Grande, Brazil, in 2004, 2005, and 2009, respectively. Since 2009, he has been a professor with the University of Brasilia, Brazil, and the Head of the Power System Protection Group. From 2019 to 2020, he was a visiting professor at the Texas A&M University, College Station, TX, US. His research interests focus on power system protection, fault location, and electromagnetic transients. He is an Editor for the IEEE Transactions on Power Delivery and Member of SC B5–Protection and Automation Committee of Cigre Brazil.

Jéssica S. G. Pena received the B.Sc. degree in energy engineering and the M.Sc. degree in electrical engineering from the University of Brasilia (UnB), Brasilia, Brazil, in 2013 and 2016, respectively. She is currently working toward the Ph.D. degree in electrical engineering at the UnB. Her research interests include power system protection, energy quality and electrical generation.

Helon D. M. Braz (M' 17) received the B.Sc. degree in electrical engineering from the Federal University of Paraíba (UFPB), Campina Grande, Brazil, in 2001. He later received his M.Sc. and Ph.D. degrees from the Federal University of Campina Grande (UFCG), Campina Grande, Brazil, in 2003 and 2010, respectively. He worked at Eletrobras Chesf on power systems planning studies for seven years and currently, he is a Professor at UFPB. His research activities are focused on optimization methods applied in power systems.

Mladen Kezunovic (S'77-M'80–SM'85–F'99-LF'17) has been with Texas A&M University, College Station, TX, USA for 35 years, where he holds titles of Regents Professor, Eugene E. Webb endowed Professor, and Site Director of "Power Engineering Research Center" consortium. He is also the Principal of XpertPower Associates™, a consulting firm specializing in power systems data analytics for the last 30 years. His expertise is in protective relaying, computational intelligence for automated power system disturbance analysis, predictive data analytics for outage management, and smart grids. Dr. Kezunovic is an IEEE Life Fellow, and a CIGRE Fellow, Honorary and Distinguished Member. He is a Registered Professional Engineer in Texas.